Scattering of electrons in graphene by clusters of impurities

M. I. Katsnelson

Institute for Molecules and Materials, Radboud University Nijmegen, Heijendaalseweg 135, 6525 AJ Nijmegen, The Netherlands

F. Guinea

Instituto de Ciencia de Materiales de Madrid (CSIC), Sor Juana Inés de la Cruz 3, Madrid 28049, Spain

A. K. Geim

Manchester Centre for Mesoscience and Nanotechnology, University of Manchester, M13 9PL Manchester, United Kingdom

It is shown that formation of clusters of charged impurities on graphene can suppress their contribution to the resistivity by a factor of the order of the number of impurities per cluster. The dependence of conductivity on carrier concentration remains linear. In the regime where the cluster size is large in comparison to the Fermi wavelength, the scattering cross section shows sharp resonances as a function of incident angle and electron wave vector. In this regime, due to the dominant contribution of scattering by small angles, the transport cross section can be much smaller than the total one, which may be checked experimentally by comparison of the Dingle temperature to the electron mean-free path.

PACS number(s): 72.10.−d, 72.80.Rj, 73.61.Wp

I. INTRODUCTION

Graphene currently attracts intense attention as a novel strictly two-dimensional (2D) system with unique electronic properties that are interesting with respect to both basic physics and potential applications (for review, see Refs. 1–3). It was shown already in the early reports on graphene[4] that charge carriers in this material exhibited a remarkably high mobility μ such that submicron mean-free paths were routinely achievable and an order-of-magnitude higher μ were observed for suspended graphene samples.[5,6] Away from the neutrality point, the conductivity of graphene is weakly temperature dependent and approximately proportional to the carrier concentration n.[7,8] Despite extensive experimental and theoretical efforts, there is still no consensus about the scattering mechanism limiting μ in graphene on a substrate. Charged impurities are probably the simplest and thus the most natural candidate,[9–11] and this conjecture is in agreement with the experiments in which potassium atoms were deposited on graphene at cryogenic temperatures.[12] However, room-temperature experiments with gaseous adsorbates such as NO_2 have showed only a weak dependence of μ on charged impurity concentration.[13] The latter observation agrees with several reports of only modest changes observed in μ after thermal annealing of spuriously doped samples. Furthermore, recent experiments[14] did not find any significant dependence of μ on immersing graphene devices in high-κ media such as ethanol and water (dielectric constants of $\kappa \approx 25$ and 80, respectively) but this also disagrees with another report[15] in which two monolayers of ice increased μ in graphene by $\approx 30\%$. Because of the experimental controversy, alternative mechanisms such as scattering on frozen ripples[16] and resonant impurities[17,18] were discussed.

Regardless of the experimental debate about the dominant scattering mechanism, the case of graphene covered with adsorbates at elevated temperatures[12] generally requires more careful consideration since there is a vast literature which shows the formation of clusters of different metals on the surface of graphite.[19–24] These atoms easily diffuse on graphite's surface overcoming only relatively low barriers and tend to form clusters. Potassium atoms on graphite arrange themselves into the so-called $p(2 \times 2)$ structure with a K-K spacing of 0.492 nm, that is, roughly, 3.5 nearest-neighbor carbon-carbon distances.[22] However, in the case of graphite, this usually happens only at low temperatures and high coverage by adsorbates.[22] For low-doping concentrations such as those used in typical experiments on graphene, adsorbates on graphite are randomly dispersed and, at elevated temperatures, evaporate from its surface, except for such materials as, for example, Au, that forms stable clusters on graphite.

From the surface science perspective, graphene is different from graphite, and we expect that clusters can be more easily formed on graphene and be stable at high temperatures. Indeed, it was shown experimentally[13] that graphene binds such molecules as NO_2, NH_2, and H_2O, etc. even at room temperature. In the case of graphite, they can attach only below liquid-nitrogen temperatures.[22] The reason for the stronger attachment remains unclear but could be due to the presence of ripples on graphene.[25] According to both experiments and theory,[26] ripples can bind even atomic hydrogen that is unstable on a flat surface on both graphene and graphite.

We believe that once attached to graphene (and this certainly happens for various gases even at room temperature), adsorbates should tend to cluster, much more so than for the case of graphite's surface. First, ripples would obviously force them to move from the valleys onto the hills which favor the adsorption. Second, there exists an additional long-range attraction due to Casimir-type interaction mediated by Dirac fermions,[27] which is absent for graphite.

On the basis of the above consideration that agrees with what is now known about graphene adsorbates, both theoretically and experimentally, it is important to consider how such clustering of adsorbates can influence the electronic properties of graphene. In this paper, we analyze the scattering of Dirac fermions by clusters of charged impurities and

show that for the same doping level such a disorder results in significantly lower resistivity. This model reconciles the doping experiments at cryogenic[12] and ambient[13] conditions, as low temperatures prevent surface diffusion and, therefore, clustering of adsorbates.

Section II presents the model to be studied. Section III contains the main results. We discuss in Sec. IV possible extensions of the model. The main conclusions are described in Sec. V.

II. MODEL

Let us first assume that the charged impurities inside the cluster are ordered, occupying positions over the centers of carbon hexagons, as in the $p(2 \times 2)$ structure mentioned above.[22] In such a situation the impurities do not break the sublattice symmetry and cannot lead therefore to the gap opening. The main effect is therefore merely a local doping of graphene, that is, shift of its chemical potential, similar to what happens for graphene on the top of metals.[28] Another effect, that is, the residual unscreened Coulomb potential, of the cluster as a whole, $\sim 1/r$, far from the cluster, will be discussed further.

We start with the simplest model, that is, the scattering of the charge carriers by a closed region where the chemical potential has been modified. For simplicity, we assume a circular cluster. The problem of scattering of the 2D massless Dirac electrons by the circularly symmetric potential well has been considered in Refs. 17 and 29–33. The model parameters are the Fermi energy and Fermi wave vector outside the cluster, ϵ_F and k_F, the change in chemical potential inside the cluster, V, the Fermi velocity, v_F, and the radius of the cluster, R. We take $\hbar = 1$ in the following. The differential cross section can be written in terms of Bessel functions, whose dimensionless arguments are $\phi_{\text{out}} = k_F R$ and $\phi_{\text{in}} = (k_F + V/v_F)R$. We assume that the cluster is heavily doped so that $\phi_{\text{in}} \gg \phi_{\text{out}}$. The charge induced inside the cluster is estimated as $\pi(VR)^2 v_F^{-2} \propto \phi_{\text{in}}^2$. We will neglect the intervalley scattering, which is justified if the boundaries of the cluster are smooth on the atomic scale, and $R \gg a$, where a is the lattice constant.

III. RESULTS

The scattering cross section reads[17,29–33]

$$\sigma(\theta) = \frac{4}{\pi k_F}|f(\theta)|^2 \quad f(\theta) = \sum_{n=-\infty}^{n=\infty} \frac{R_n e^{in\theta}}{i + R_n},$$

$$R_n = -\frac{J_n(\phi_{\text{out}})J_{n+1}(\phi_{\text{in}}) - J_{n+1}(\phi_{\text{out}})J_n(\phi_{\text{in}})}{Y_n(\phi_{\text{out}})J_{n+1}(\phi_{\text{in}}) - Y_{n+1}(\phi_{\text{out}})J_n(\phi_{\text{in}})}. \quad (1)$$

Note that since $R_n = R_{-1-n}$, the back-scattering amplitude vanishes, $f(\theta = \pi) = 0$ which is the consequence of the pseudospin conservation at the "chiral" scattering related with the Klein paradox.[34]

The cross section shows two regimes depending on whether $\phi_{\text{out}} = k_F R \ll 1$ or $\phi_{\text{out}} \gg 1$. In the first case, the cluster is small compared to the Fermi wavelength. The cluster per-
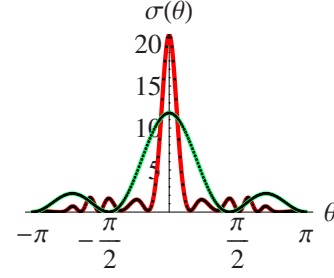

FIG. 1. (Color online) Angular dependence of the cross section, $\sigma(\theta)$, in nanometers, for a cluster of radius $R = 20$ nm with a chemical potential of $V = 500$ meV. (Red, narrow peak): charge density $\rho = 5 \times 10^{12}$ cm^{-2} ($E_F = 250$ meV, $k_F R = 7.9$). (Green, wide peak): angular dependence of the cross section (multiplied by 100) for $\rho = 10^{10}$ cm^{-2} ($E_F = 11$ meV, $k_F R = 0.35$).

turbs weakly the electronic wave functions and the Born approximation can be used. The differential cross section, $\sigma(\theta)$ has in this case a weak dependence on the scattering angle θ. The total cross section increases as k_F increases, $\sigma \sim [V/(v_F R^{-1})]^2 k_F R^2$.

For $k_F R \gg 1$, the cross section as a function of the incident angle θ shows a narrow maximum at $\theta = 0$. In addition, both the angular resolved and the integrated cross sections show resonances associated to quasibound states inside the cluster. The integrated cross section decays slowly as a function of k_F. The angular dependence of the cross section is shown in Fig. 1.

Results for the transport cross section, $\sigma_{\text{tr}} = \int_{-\pi}^{\pi} \sigma(\theta)[1 - \cos(\theta)]d\theta$, are shown in Fig. 2. We analyze in Fig. 2 the total cross section for t, $V = 0.5$ eV, which describes the shift in chemical potential due to weakly coupled adsorbates such as Al, Ag, or Cu.[28] Similar results, although with a smaller periodicity, are found for $V = 2$ eV, which describes strongly coupled adsorbates, such as K, where the charge transfer can reach $\frac{1}{8}$ per carbon atom.[35] The radius of the cluster was chosen as $R = 20$ nm, which is comparable to the size in ripples found in graphene.[25] The total number of electrons inside the cluster is therefore $N_{\text{in}} = \pi \rho R^2 \approx 250$, where ρ is the charge density inside the cluster, $\rho = k_F^{\text{cl}2}/\pi$, $v_F k_F^{\text{cl}} = V$.

The limit $k_F R \gg 1$ can be analyzed by using the asymptotic expressions for the Bessel functions at $x \to \infty$,

$$J_n(x) + iY_n(x) \approx \sqrt{\frac{2}{\pi x}} e^{i[x - (n\pi/2) - (\pi/4)]}. \quad (2)$$

Then, the expression for the reflection coefficient in radial waves, r_n (see Ref. 33) simplifies to
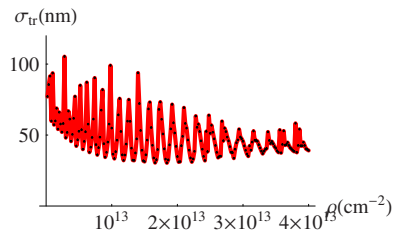

FIG. 2. (Color online) Integrated transport cross section σ_{tr} for a cluster of radius $R = 20$ nm and a shift in the chemical potential of $V = 0.5$ eV.
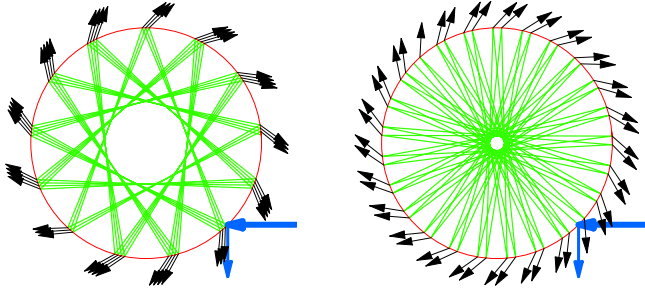
FIG. 3. (Color online) Classical trajectories of an electron scattered by a circular cluster. 50 internal reflections are shown. The impact angle, θ, of the incoming trajectories is $\theta = \pi/4$. Left: $V = E_F$. Right: $V = 10 E_F$.

$$r_n \approx \begin{cases} \tan(\phi_{\text{in}} - \phi_{\text{out}}) = \tan\left(\dfrac{VR}{v_F}\right) & n \ll \phi_{\text{in}} \\ 0 & n \gg \phi_{\text{in}}, \end{cases} \tag{3}$$

and the cross section can be approximated as

$$\sigma(\theta) \approx \sum_{n=-n_{\max}}^{n=n_{\max}} \sum_{n'=-n_{\max}}^{n'=n_{\max}} \frac{4\left|\sin\left(\dfrac{VR}{v_F}\right)\right|^2}{\pi k_F} e^{i(n-n')\theta}, \tag{4}$$

where $n_{\max} \sim k_F R$. The transport cross section in this regime is

$$\sigma_{\text{tr}} = \int_{-\pi}^{\pi} \sigma(\theta)[1-\cos(\theta)]d\theta \propto \frac{\left|\sin\left(\dfrac{VR}{v_F}\right)\right|^2}{k_F}. \tag{5}$$

The scattering process in this limit can be studied by the methods of geometrical optics.[32,36,37] Typical trajectories as a function of the shift in potential inside the cluster and impact angle are shown in Fig. 3. The scattering will be dominated by periodic orbits inside the cluster. These periodic orbits are the semiclassical analogs of the resonances of the quantum model. For energies such that the internal trajectories are not periodic, the transmitted waves will interfere destructively. A periodic trajectory will lead to transmitted rays at well-defined angles, as found in the full calculation of $\sigma(\theta)$. Typical trajectories as function of the shift in potential inside the cluster and impact angle are shown in Figs. 3 and 4. The only periodic orbits for large values of V/E_F include many inter-
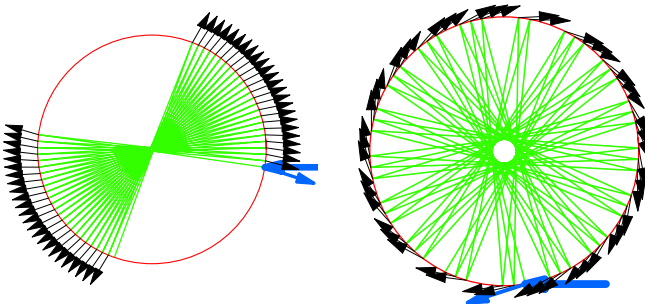

FIG. 4. (Color online) As in Fig. 3, for $V = 10 E_F$, as a function of the impact angle. Left: $\theta = \pi/20$. Right: $\theta = \pi/2 - \pi/20$.

nal reflections, which correspond to high angular momenta in the quantum model. These orbits are probably less efficient in modifying the scattering process than the orbits with a lower number of internal reflections, leading to the calculated cross section, with a sharp maximum as a function of the incident angle. Note that the resonances under discussion are two-dimensional analogs of the "Fabry-Perot" resonances in the Klein tunneling regime.[34]

The elastic electron mean-free path, l, is given approximately by

$$l \sim \frac{1}{n_C \sigma_{\text{tr}}}, \tag{6}$$

where n_C is the cluster concentration. At low carrier densities, $k_F R \ll 1$, the Born approximation gives

$$\sigma_{\text{tr}} \propto k_F R^2 \left(\frac{V}{v_F R^{-1}}\right)^2 \tag{7}$$

and σ_{tr} is proportional to the density of states and to the square of the potential. At high densities, $k_F R \gg 1$, one can use Eq. (5). The conductivity is estimated as

$$g = \frac{e^2}{h} k_F l \sim \begin{cases} \dfrac{e^2}{h} \dfrac{1}{n_C R^2} \left(\dfrac{v_F R^{-1}}{V}\right)^2 & k_F R \ll 1 \\ \dfrac{e^2}{h} \dfrac{k_F^2}{n_C} & k_F R \gg 1. \end{cases} \tag{8}$$

We expect the oscillations of the cross section shown in Fig. 2 to be averaged out in clusters with less symmetric shapes. The parameter $k_F R$ reaches the value $k_F R \approx 10\text{–}12$ for $R = 20$ nm and charge density in the clean regions $\rho = 2 \times 10^{13}$ cm^{-2}.

Interestingly, for the regime $\phi_{\text{out}} \gg 1$ the total cross section σ_{tot} distinguished from σ_{tr} by the absence of the factor $1 - \cos\theta$ in Eq. (5) is larger than σ_{tr} by a factor $k_F R$. The total cross section is related with the single-particle decoherence time which determines, e.g., Dingle temperature in the Shubnikov–de Haas oscillations.[38]

The elastic mean-free path depends on the cluster density and carrier concentration, ρ. For $n_C = 10^{10}$ cm^{-2} and $\rho = 5 \times 10^{12}$ cm^{-2} we obtain $l = 1/(n_C \sigma) \approx 200$ nm.

We have neglected so far the long-range part of the Coulomb potential induced by the cluster. This potential will modify the scattering cross section for electron wavelengths $k_F^{-1} \gtrsim R$. The cross section will depend on the carrier concentration as $\sigma_{\text{tr}} \propto k_F^{-1}$.[31,39–41] As a result, we expect that the conductivity for $k_F R \ll 1$ will scale as k_F^2,[11,42] instead of the dependence given by Eq. (8). However, since the scattering cross section is proportional, in Born approximation, to the charge square and to the first power of the charge concentration, the clusterization will lead to the suppression of this contribution to the resistivity by a factor of order of number of atoms in cluster in comparison with the case of chaotically distributed impurities.

IV. BEYOND THE SIMPLIFIED MODEL

Our model of completely ordered impurities inside the cluster is oversimplified. However, if disorder inside the cluster is relatively weak so that the *local* mean-free path l
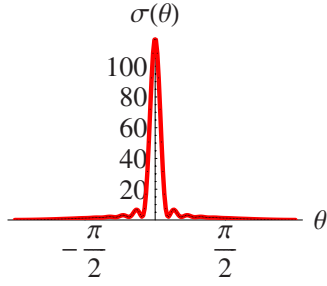
FIG. 5. (Color online) Angular dependence of the cross section when the cluster is determined by a mass term, which breaks the symmetry between the sublattices. The parameters used are $kR = 10$ and $\Delta R/v_F = 20$.

exceeds the electron wavelength inside the cluster $\lambda \approx h v_F/V$, one can expect that above consideration is correct, at least, qualitatively (the local mean-free path is defined here as the mean-free path of the infinite-disordered system with the same chemical potential and the same distribution of the scattering potential as inside the cluster). If the disorder becomes stronger one reaches at some moment the Mott limit $l \approx \lambda$ without further localization, due to the Klein tunneling.[34] In this regime, the electron rays inside the cluster are no more straight and the Fabry-Perot resonances are destroyed. The cluster with such strong disorder will behave just as an obstacle of size R with the transport cross section of order of R.

Another effect which should be considered is a possible formation of superstructure inside the cluster. It can break the sublattice equivalence and lead to the local gap opening. To see potential consequences of this local reconstruction of the electronic structure, one can extend the model to the case when the cluster is defined by a mass term rather than a shift of chemical potential. Similar boundary conditions were discussed in Ref. 43. We assume that the mass, Δ, is only finite inside the cluster. We also neglect, for simplicity, the shift of the chemical potential. The cross section in such model is expressed in terms of the new reflection amplitudes [cf. Eq. (1)],

$$R_n = -\frac{ia_- J_n(k_F R) I_{n+1}(\kappa R) - a_+ J_{n+1}(k_F R) I_n(\kappa R)}{ia_- Y_n(k_F R) I_{n+1}(\kappa R) - a_+ Y_{n+1}(k_F R) I_n(\kappa R)},$$

$$\kappa = \frac{\sqrt{\Delta^2 - (E_F + V)^2}}{v_F}, \quad a_\pm = \sqrt{\frac{1}{2} \pm \frac{\Delta}{2E}}, \qquad (9)$$

where $I_n(x)$ is a modified Bessel function, which is zero at the origin and grows exponentially as $x \to \infty$.

We have also calculated the cross section including a staggered potential, Δ. The main effect of a mass term seems to be to reduce the oscillations of the transport cross section as a function of angle. If the mass term is large enough, the effect should be qualitatively the same as for the strong disorder, that is, the transport cross section will be of the order of R, as for a nontransparent obstacle in optics. The changes induced by a mass term in the differential cross section are shown in Fig. 5.

V. CONCLUSIONS

Let us summarize the main results of our consideration. (i) The transport cross section of charge carriers in graphene by large neutral clusters due to a shift of the chemical potential inside the cluster becomes independent of the cluster size, R, and shift in chemical potential, V, for $k_F R \gg 1$, except for an oscillatory function. This can be viewed as a consequence of the Klein tunneling;[34] electrons can always tunnel into the cluster, irrespective of the value of V. The oscillatory function is, most likely, replaced by its average for clusters with irregular shapes, as one can assume by analogy with the geometric optics.[44] (ii) The total scattering cross section, obtained by integrating $\sigma(\theta)$ over angles, is proportional to R for $k_F R \gg 1$, as it should. In this regime $\sigma_{tot}/\sigma_{tr} \approx k_F R \gg 1$ which, in principle, can be observed by the comparison of the mean-free path with the Dingle temperature if this scattering mechanism is dominant. For all other scattering mechanisms considered before, including charged impurities, $\sigma_{tot} \approx \sigma_{tr}$, with a numerical factor of order of 1. (iii) The transport cross section is proportional to k_F^{-1}. Hence, scattering by large clusters leads to a dependence on carrier density similar to that for charged impurities or resonant scatterers, $g \propto n$. (iv) The main difference in the expression for the conductivity between scattering by neutral clusters and scattering by charged impurities is that the impurity concentration has to be replaced by the cluster concentration which increases the electron mobility, roughly, by 2 orders of magnitude. Thus, possible clusterization of charged impurities in graphene can probably explain the relatively weak dependence of the mobility on charge impurity concentration[13] and dielectric constant.[14] (v) The formation of clusters is a process favored by high atomic diffusion. Hence, we expect that by annealing the samples used in Ref. 12 above 100 K, the mobility will increase toward the values measured before doping by potassium. (vi) The correlation observed in Ref. 45 between the shift of the Dirac point and the electron mobility for different adsorbates as a function of adsorbate concentration is consistent with the formation of clusters. The effective charge, q_i^*, transferred from the adsorbate atom to the graphene layer varies for different adsorbates. For elements that transfer to graphene an amount of charge much less than one-electron charge, such as Pt, the scattering cross section[31] goes as q_i^{*2}. The shift of the Dirac point should be proportional to $E_{D_i} \propto n_i q_i^*$, where n_i is the concentration of the adsorbate. The change in mobility should scale, on the other hand, as $\mu_i^{-1} \propto n_i q_i^{*2}$. For adsorbates such that $q_i^* \approx 1e$, the mobility scales as $\mu_i^{-1} \propto n_i q_i^*$. Hence, different adsorbates should show different ratios μ_i^{-1}/E_{D_i}. A ratio that varies weakly for different adsorbates is more consistent with the existence of clusters, each of which transfers to graphene a few free-electron charges independent of the type of adsorbate and size of the cluster.

---

[1] A. K. Geim and K. S. Novoselov, Nature Mater. **6**, 183 (2007).

[2] M. I. Katsnelson, Mater. Today **10**, 20 (2007).

[3] A. H. Castro Neto, F. Guinea, N. M. R. Peres, K. S. Novoselov, and A. K. Geim, Rev. Mod. Phys. **81**, 109 (2009).

[4] K. S. Novoselov, A. K. Geim, S. V. Morozov, D. Jiang, Y. Zhang, S. V. Dubonos, I. V. Grigorieva, and A. A. Firsov, Science **306**, 666 (2004).

[5] K. I. Bolotin, K. J. Sikes, Z. Jiang, M. Klima, G. Fudenberg, J. Hone, P. Kim, and H. L. Stormer, Solid State Commun. **146**, 351 (2008).

[6] X. Du, I. Skachko, A. Barker, and E. Y. Andrei, Nat. Nanotechnol. **3**, 491 (2008).

[7] K. S. Novoselov, A. K. Geim, S. V. Morozov, D. Jiang, M. I. Katsnelson, I. V. Grigorieva, S. V. Dubonos, and A. A. Firsov, Nature (London) **438**, 197 (2005).

[8] Y. Zhang, Y.-W. Tan, H. L. Stormer, and P. Kim, Nature (London) **438**, 201 (2005).

[9] K. Nomura and A. H. MacDonald, Phys. Rev. Lett. **96**, 256602 (2006).

[10] T. Ando, J. Phys. Soc. Jpn. **75**, 074716 (2006).

[11] S. Adam, E. H. Hwang, V. Galitski, and S. Das Sarma, Proc. Natl. Acad. Sci. U.S.A. **104**, 18392 (2007).

[12] J. H. Chen, C. Jang, S. Adam, M. S. Fuhrer, E. D. Williams, and M. Ishigami, Nat. Phys. **4**, 377 (2008).

[13] F. Schedin, A. K. Geim, S. V. Morozov, E. W. Hill, P. Blake, M. I. Katsnelson, and K. S. Novoselov, Nature Mater. **6**, 652 (2007).

[14] L. A. Ponomarenko, R. Yang, T. M. Mohiuddin, S. M. Morozov, A. A. Zhukov, F. Schedin, E. W. Hill, K. S. Novoselov, M. I. Katsnelson, and A. K. Geim, arXiv:0809.1162 (unpublished).

[15] C. Jang, S. Adam, J.-H. Chen, E. D. Williams, S. Das Sarma, and M. S. Fuhrer, Phys. Rev. Lett. **101**, 146805 (2008).

[16] M. I. Katsnelson and A. K. Geim, Philos. Trans. R. Soc. London, Ser. A **366**, 195 (2008).

[17] M. I. Katsnelson and K. S. Novoselov, Solid State Commun. **143**, 3 (2007).

[18] T. Stauber, N. M. R. Peres, and F. Guinea, Phys. Rev. B **76**, 205423 (2007).

[19] R. D. Diehl and R. McGrath, Surf. Sci. Rep. **23**, 43 (1996).

[20] C. Binns, S. H. Baker, C. Demangeat, and J. C. Parlebas, Surf. Sci. Rep. **34**, 107 (1999).

[21] D. Q. Yang and E. Sacher, Surf. Sci. **516**, 43 (2002).

[22] M. Caragiu and S. Finberg, J. Phys.: Condens. Matter **17**, R995 (2005).

[23] H. Hovel and I. Barke, Prog. Surf. Sci. **81**, 53 (2006).

[24] K. T. Chan, J. B. Neaton, and M. L. Cohen, Phys. Rev. B **77**, 235430 (2008).

[25] J. C. Meyer, A. K. Geim, M. I. Katsnelson, K. S. Novoselov, T. J. Both, and S. Roth, Nature (London) **446**, 60 (2007).

[26] D. C. Elias, R. R. Nair, T. M. G. Mohiuddin, S. V. Morozov, P. Blake, M. P. Halsall, A. C. Ferrari, D. W. Boukhvalov, M. I. Katsnelson, A. K. Geim, and K. S. Novoselov, Science **323**, 610 (2009).

[27] A. Shytov, D. Abanin, and L. Levitov, arXiv:0812.4970 (unpublished).

[28] G. Giovannetti, P. A. Khomyakov, G. Brocks, V. M. Karpan, J. van den Brink, and P. J. Kelly, Phys. Rev. Lett. **101**, 026803 (2008).

[29] P. M. Ostrovsky, I. V. Gornyi, and A. D. Mirlin, Phys. Rev. B **74**, 235443 (2006).

[30] M. Hentschel and F. Guinea, Phys. Rev. B **76**, 115407 (2007).

[31] D. S. Novikov, Phys. Rev. B **76**, 245435 (2007).

[32] J. Cserti, A. Pályi, and C. Péterfalvi, Phys. Rev. Lett. **99**, 246801 (2007).

[33] F. Guinea, J. Low Temp. Phys. **153**, 359 (2008).

[34] M. I. Katsnelson, K. S. Novoselov, and A. K. Geim, Nat. Phys. **2**, 620 (2006).

[35] M. S. Dresselhaus and G. Dresselhaus, Adv. Phys. **30**, 139 (1981).

[36] V. V. Cheianov, V. Fal'ko, and B. L. Altshuler, Science **315**, 1252 (2007).

[37] J. L. Garcia-Pomar, A. Cortijo, and M. Nieto-Vesperinas, Phys. Rev. Lett. **100**, 236801 (2008).

[38] D. Schönberg, *Magnetic Oscillations in Metals* (Cambridge University Press, Cambridge, England, 1984).

[39] A. V. Shytov, M. I. Katsnelson, and L. S. Levitov, Phys. Rev. Lett. **99**, 236801 (2007).

[40] M. M. Fogler, D. S. Novikov, and B. I. Shklovskii, Phys. Rev. B **76**, 233402 (2007).

[41] V. M. Pereira, J. Nilsson, and A. H. Castro Neto, Phys. Rev. Lett. **99**, 166802 (2007).

[42] K. Nomura and A. H. MacDonald, Phys. Rev. Lett. **98**, 076602 (2007).

[43] M. V. Berry and R. J. Mondragon, Proc. R. Soc. London, Ser. A **412**, 53 (1987).

[44] B. Dietz and U. Smilansky, Chaos **3**, 581 (1993).

[45] K. Pi, K. M. McCreary, W. Bao, W. Han, Y. F. Chiang, Y. Li, S.-W. Tsai, C. N. Lau, and R. K. Kawakami, arXiv:0903.2837 (unpublished).